Journal of Applied Polymer Science

Influence of Metal-Oxide-Supported Bentonites on the Pyrolysis Behavior of Polypropylene and High-Density Polyethylene

Imtiaz Ahmad,[1] Mohammad Ismail Khan,[1] Hizbullah Khan,[2] Mohammad Ishaq,[1] Razia Tariq,[1] Kashif Gul,[1] Waqas Ahmad[1]

[1]Institute of Chemical Sciences, University of Peshawar, Peshawar, Khyber Pakhtunkhwa 25120, Pakistan
[2]Department of Environmental Sciences, University of Peshawar, Peshawar, Khyber Pakhtunkhwa 25120, Pakistan
Correspondence to: I. Ahmad (E-mail: patwar2001@yahoo.co.in)

ABSTRACT: In this article, we report on the pyrolysis of polypropylene (PP) and high-density polyethylene (HDPE) in the absence and presence of plain and metal-oxide-impregnated bentonite clays [BCs; acid-washed bentonite clay (AWBC), Zn/AWBC, Ni/AWBC, Co/AWBC, Fe/AWBC, and Mn/AWBC] into useful products. Thermal and catalytic runs were performed at 300°C in the case of PP and at 350°C in the case of HDPE for a contact time of 30 min. The effects of different catalysts and their concentrations on the overall yields and the yields of liquid, gas, and residue were studied. The efficacy of each catalyst is reported on the basis of the highest liquid yields (in weight percentage). The derived liquid products were analyzed by Fourier transform infrared spectroscopy and gas chromatography–mass spectroscopy; this confirmed the presence of paraffins, olefins, and naphthenes. The results indicate the catalytic role of impregnated BCs compared to plain BC with the optimum efficiency shown by Co/AWBC in the case of PP and Zn/AWBC in the case of HDPE toward the formation of liquid products in a desirable C range with the enrichment of olefins and naphthenes in the case of PP and paraffins and olefins in the case of HDPE compared to the thermal run. © 2014 Wiley Periodicals, Inc. J. Appl. Polym. Sci. **2015**, *132*, 41221.

KEYWORDS: catalysts; degradation; polyolefins

Received 14 February 2014; accepted 24 June 2014
DOI: 10.1002/app.41221

INTRODUCTION

There is a dire need to develop and deploy new environmentally friendly and cost-effective plastic waste management technologies as currently used disposal options become less viable. Among these, conversion to energy resources has been a significant way to use such waste streams effectively and to meet with the growing demand from the energy sector. Extensive research is underway worldwide for the production of alternative fuels from industrial and household waste plastic streams through the use of heat only (thermal pyrolysis) and both heat and chemicals (catalytic pyrolysis).[1–5]

Catalytic pyrolysis is considered to be the most promising route because of several benefits over the thermal pyrolysis.[6–8] A number of heterogeneous catalysts has been studied previously to evaluate their effectiveness in the conversion of plastics into value-added products such as kerosene, diesel fuel oil, naphtha, engine oil, and fuel oil.[9–14] It has been reported elsewhere that both the physical and chemical properties of catalysts influence their activities toward polymer degradation. Among the physical properties (e.g., surface area, particle size, pore volume, pore size distribution, pore structure, shape-selective effect) and chemical properties (e.g., Lewis and Brönsted acidities) have been reported to be the important factors.[15–19]

Pillared clays are enjoying popularity as catalysts in a various industrial processes, including cracking, hydroisomerization, dehydration, dehydrogenation, hydrogenation, aromatization, disproportionation, esterification, alkylation, selective catalytic and reduction,[20] because of their textural and chemical properties. Among this class of catalysts, bentonite clays (BCs) have been the focus of many researchers in the hydrocracking of heavy fuel oils and getting bio-oil from the copyrolysis of biomass and polyethylene.[21,22] Different types of BCs, named after their respective dominant elements, such as potassium (K), sodium (Na), calcium (Ca), and aluminum (Al), have been reported only recently as catalysts for polymer degradation.[23] However, the use of metal-oxide-impregnated BCs as catalysts or supports for plastic degradation has not been reported yet.

This study was aimed at the evaluation of the catalytic activities of plain (Al–Si dominant) and various metal-oxide-impregnated BCs in the pyrolytic conversion of polyolefins [polypropylene (PP) and high-density polyethylene (HDPE)] into useful products. The influence of each catalyst on product distribution in

terms of the yields of end products, particularly liquid products, is described. The selectivity of catalysts in terms of C number (C_6 to more than C_{30} hydrocarbons) and hydrocarbon group type distributions (paraffins, naphthene, olefins, and aromatics) in the liquid products is also reported.

EXPERIMENTAL

Chemicals and Reagents

All chemicals used were analytical grade (Merck) and were used without further purification. Nitrogen gas (99% purity) was purchased from British Oxygen Co. (Peshawar, Pakistan). The model polyolefins (i.e., PP and HDPE) were purchased from the local market. BC was provided by Pakistan Mineral Development Corp., Government of Khyber Pakhtunkhwa. The different transition-metal salts used in impregnation included $FeCl_3$ (79%), $CoCl_2$ (99%), Zn $(NO_3)_2{\cdot}6H_2O$ (98%), $MnCl_2{\cdot}4H_2O$ (99%), and Ni $(NO_3)_2{\cdot}6H_2O$ (99%).

The proximate analyses, that is, moisture, ash, volatile matter, and fixed carbon (weight percentage), and ultimate analyses, that is, carbon, hydrogen, nitrogen, sulfur, and oxygen (weight percentage), of the feed polymers were determined according to ASTM Standards/Institute of Petroleum designated methods (Table I).

Table I. Properties of Feed Polyolefins

	Parameter (wt %)	
	PP	HDPE
Proximate analysis (ASTM D 3173-75)		
Moisture (ASTM D 3173)	0.00	0.00
Volatile matter (ASTM D 3173)	99.90	99.81
Ash (ASTM D 3174)	0.01	0.18
Fixed carbon (ASTM D 3172-89)	0.09	0.01
Carbon residue (ASTM D 189)	0.20	0.61
Ultimate analysis (ASTM D 5291)		
Carbon	83.10	84.74
Hydrogen	11.77	11.65
Nitrogen	0.14	0.02
Sulfur	0.16	0.66
Thermal analysis		
Decomposition temperature (°C)	405	590

Preparation of the Plain (Acid-Washed) and Transition-Metal-Impregnated BCs [Acid-Washed Bentonite Clay (AWBC), Zn/AWBC, Ni/AWBC, Co/AWBC, Fe/AWBC, and Mn/AWBC]

Procedure. Before impregnation, the raw BC was modified with acid with a procedure reported elsewhere.[24] BC (50 g) was placed in a 250-mL, round-bottomed flask, and 150 mL of a 0.1*N* HCl solution was added. The suspension was heated under reflux for a time duration of 3 h with continuous stirring and filtered. The residue was washed with a copious amount of distilled water until it was free of acid, dried in an oven at 100°C for 12 h, ground into a fine powder, and sieved through a 125-μm screen. AWBC was then calcined at 550°C for 5–6 h in an air supply in a muffle furnace, stored in a glass vial, and used as such in metal impregnation.

Impregnation. Metal impregnation on AWBC was performed with the incipient wetness method.[25] In a typical run, a stoichiometric quantity of metal salt was weighed and dissolved in 100 mL of deionized water in a 250-mL beaker, to which 3 g of AWBC was added and stirred at 65°C for 4 h. The suspension was dried in an oven maintained at 100°C until a constant mass was reached. The dried mass was crushed, calcined in a plentiful supply of air at 500°C for 4 h in a muffle furnace, and stored for further activity tests. In this way, metal-oxide-impregnated AWBCs were prepared.

Catalyst Characterization

The acid-modified and various metal-impregnated AWBCs were characterized. The textural properties of each catalyst were studied by scanning electron microscopy (SEM; JEOL JSM-5910, Japan). The surface properties, including surface area, pore volume, and pore diameter, were determined by a surface area analyzer (Quantachrome, Nova Station, A) with nitrogen adsorption–desorption isotherms. Phase analysis was carried out with an X-ray diffractometer (JEOL model JDX-9C, Japan) at room temperature, with Cu Kα radiation and a nickel filter.

The mineralogical analysis was carried out with a gravimetric method for the determination of Al_2O_3 and SiO_2[26] and with an atomic absorption spectrophotometer (model SENSAA dual, GBC Scientific Equipment, Australia) for Mg, Fe, Zn, Co, Ni, and Mn.

Na, K, and Ca were determined by a flame photometer (model 360, Sherwood Scientific, Ltd., United Kingdom).

Pyrolysis Experiments

Pyrolysis experiments were carried out with and without catalysts separately in a nonsweeping environment of nitrogen under optimized conditions of temperature (300°C in the case of PP and 350°C in the case of HDPE) and time (30 min). All of the experiments were carried out in triplicate, and the mean values of the overall yields and yields of liquid, gas, and coke are reported.

Pyrolysis Equipment. The pyrolysis equipment used is provided in Figure 1. The assembly consisted of a stainless steel reactor (25.4 cm length × 2.1 cm diameter), a nitrogen gas supply, a tube furnace, a Liebig condenser, water circulation (inlet and outlet), a receiving flask, and a gas exit.

Process. In a typical run, 2 g of the feed plastic was placed in the reactor, which was then screwed tightly. The reactor was connected to a nitrogen supply and purged to flush out the air present inside the reactor. The reactor was placed horizontally in a tube furnace and heated at a rate of 20°C/min up to the selected temperature. During heating, the pyrolysates/vapors leaving the reactor were allowed to flow through a water cooled condenser/gas–liquid separator. The cooling was done through water circulation. The condensates (liquid) were collected in a receiving flask. The uncondensed products (gas) were sent to a vent. We determined the yields of the solid and liquid products determined by weighing the amount of each product. The overall yields and yields of liquid, gas, and residual coke (weight basis) were calculated.

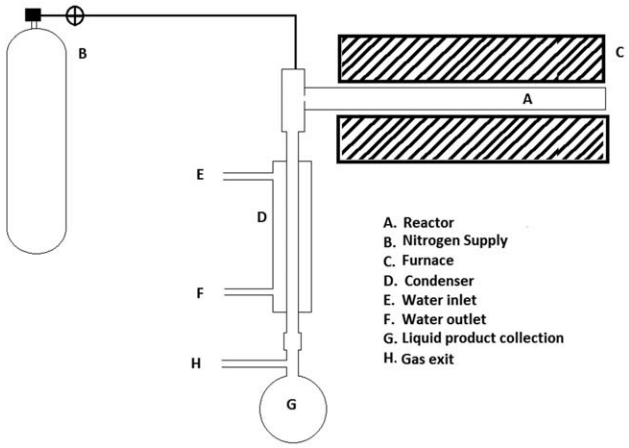

Figure 1. Schematic of the pyrolysis reactor: (A) stainless steel reactor (25.4 cm length × 2.1 cm diameter), (B) nitrogen gas supply, (C) tube furnace, (D) Liebig condenser, (E,F) water circulation (inlet and outlet), (G) receiving flask, and (H) gas exit.

Calculations

The overall (T) yields and yields of the liquid (L), gas (G), and coke/residue (R) were calculated as follows:

$$\text{Tyield (wt \%)} = \frac{W_p - W_R}{W_p}$$

$$\text{Lyield (wt \%)} = \frac{W_L}{W_p} \times 100$$

$$\text{Gyield (wt \%)} = 100 - [\%\,\text{L} + \%\,\text{R}]$$

$$\text{Ryield (wt \%)} = \frac{W_R}{W_p} \times 100$$

where W_P, W_L, and W_R are the weights of the feed polymer, liquid oil, and residue, respectively.

To study the influence of the catalyst type and concentration, the samples were pyrolyzed unstirred with 0.2 g of plastic loaded with a catalyst used in the concentration range 0.5–10 wt %. The optimum catalyst type and concentration were decided on the basis of highest weight percentage yields of the liquid products.

Product Analysis

The liquid products derived from the thermal and catalyzed runs (with optimum conditions) were analyzed by Fourier transform infrared (FTIR) spectroscopy and gas chromatography (GC)–mass spectroscopy (MS). FTIR analysis was performed with an FTIR spectrometer (model Prestige-21, Shimadzu, Japan) in the wave-number range 4000–400 cm^{-1}.

GC–MS analysis was carried out by a gas chromatograph coupled with an MS analyzer (model QP-2010, Shimadzu) with the conditions reported elsewhere.[27] The product peaks in the chromatograms were identified with the data of the National Institute of Standards and Technology-Mass Spectral Library (NIST-MS) library.

RESULTS AND DISCUSSION

Characterization of the Catalysts

The physical, chemical, and mineralogical characteristics of BC have a strong bearing on its catalytic activity. Its surface modification with metal oxides may result in the variation of properties, such as the surface acidity, porosity, pore volume, diameter, and cation-exchange capacity. This study involved the characterization of plain and various metal-oxide-impregnated AWBCs. The characterization of the original and impregnated AWBCs was carried out with Scanning Electron Microscopy (SEM), Brunauer, Emmett and Teller (BET), and Barrett-Joyner-Halenda (BJH) surface area measurements, X-ray diffraction, elemental analysis, and acidity measurement.

The morphological analysis of the plain and metal-impregnated AWBCs, that is, Co/AWBC and Zn/AWBC was performed to confirm that the impregnated metal oxides were dispersed effectively throughout the surface. The SEM of the plain AWBC is provided in Figure 2(a); this indicated its layered surface morphology. Several features, such as microfissures and channels, uniformly distributed throughout the surface were observed. Furthermore, some distinct and separately identifiable features, mostly in the form of grains of different sizes, were also observed. The micrographs of Co/AWBC and Zn/AWBC [Figure 2(b,c)] featured different surface morphologies compared with the plain AWBC. In addition, cracks and cavities distributed throughout the surface were observed. In the case of Co/AWBC, the surface seemed to consist of various formations such as flakes stacked upon each other, whereas in the case of Zn/AWBC, features such as spherules/particles were observed. All of these features were indicative that the precursor metal oxides were dispersed effectively onto the support.

The surface properties, that is, the surface area, pore size, and pore volume, of the catalysts under study were also studied. The results are provided in Table II. We observed from the results that the BET and BJH surface areas of the plain AWBC were found to be 89.87 and 155.65 m^2/g, respectively. The pore size and pore volume were found to be 125.56 Å and 0.46 cm^3/g, respectively. The results in the case of impregnated samples indicated that these properties altered to a greater extent and were markedly decreased upon impregnation, particularly in the case of the AWBCs. Among the impregnated AWBCs, the highest BET surface area of 36.37 m^2/g was observed in the case of Zn/AWBC, whereas the lowest BET surface area of 21.08 m^2/g was observed in the case of Mn/AWBC. Similar changes were also observed in the case of the pore size and pore volume. The pore size decreased from 125.56 Å in the case of plain AWBC to 57.77 Å in the case of Zn/AWBC. The pore volume determined in the case of the impregnated AWBCs was also found to decrease from 0.46 cm^3/g in the case of plain AWBC to 0.04 cm^3/g in the cases of Fe/AWBC and Mn/AWBC. The decreases in the surface area, pore volume, and pore size were attributed to the blinding of the micropores in the AWBC matrix because of the occupation of metal oxides.

The XRD patterns of the plain and metal-oxide-impregnated AWBCs are provided in Figure 3(a–c). The diffractogram of plain AWBC indicated the presence of montmorillonite as a major component;[28,29] montmorillonite consists of alternate layers of silica tetrahedral sheets and aluminum octahedral sheets interconnected by hydroxyl sheets.[29] The other minerals identified were kaolinite, quartz, and illite.[30] The XRD patterns of the impregnated AWBCs were identical to those of the plain

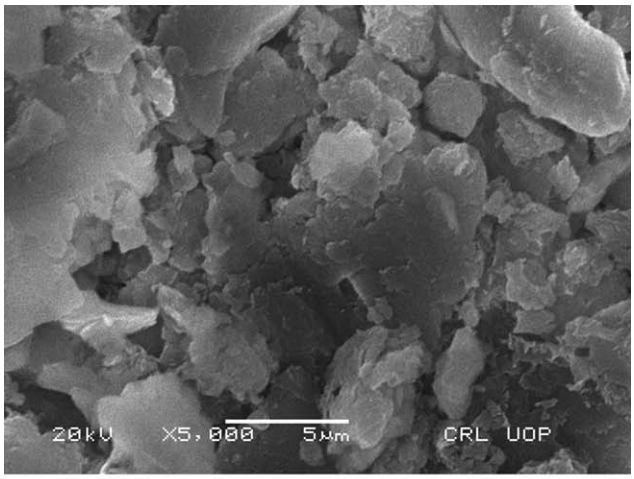

(a)

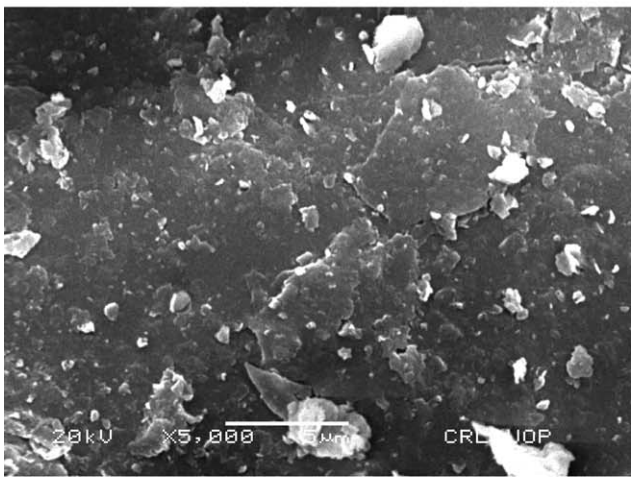

(b)

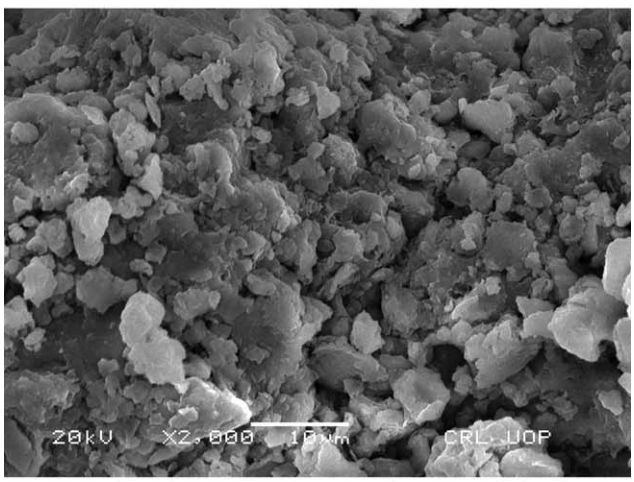

(c)

Figure 2. SEM micrographs of the original and metal-oxide-impregnated AWBCs: (a) AWBC, (b) Co/AWBC, and (c) Zn/AWBC.

Table II. Surface Properties of the Original and Metal-Oxide-Impregnated AWBCs

	Surface area (m^2/g)			
Catalyst	BET	BJH	Pore volume (cm^3/g)	Pore size (Å)
AWBC	89.87	155.65	0.46	125.56
Ni/AWBC	24.88	52.02	0.14	77.99
Co/AWBC	23.09	28.14	0.06	76.26
Fe/AWBC	24.23	22.36	0.04	75.30
Mn/AWBC	21.08	19.42	0.04	76.81
Zn/AWBC	36.37	73.05	0.14	57.77

clay. However, some additional peaks were observed, which corresponded to metal oxide. The diffractogram of Zn/AWBC showed characteristic peaks corresponding to ZnO.[31] Similarly, that of Co/AWBC indicated that the characteristic peaks corresponded to the crystalline planes of Co_2O_3.[32]

We concluded that during calcination, the metal precursors, that is, Co and Zn, were converted to their respective oxides, that is, ZnO and Co_2O_3.

Mineralogical analyses of the plain and impregnated AWBCs were also carried out. The results are provided in Table III. We also observed that the plain AWBC contained SiO_2 and Al_2O_3 in high concentrations. Other elements, K, Mg, Ca, Na, and Fe, were also found but in low concentrations. The results further indicate that the plain AWBC contained no transition metals. Mineralogical analyses of the metal-impregnated AWBCs, Co/AWBC, Zn/AWBC, Ni/AWBC, Fe/AWBC, and Mn/AWBC, were

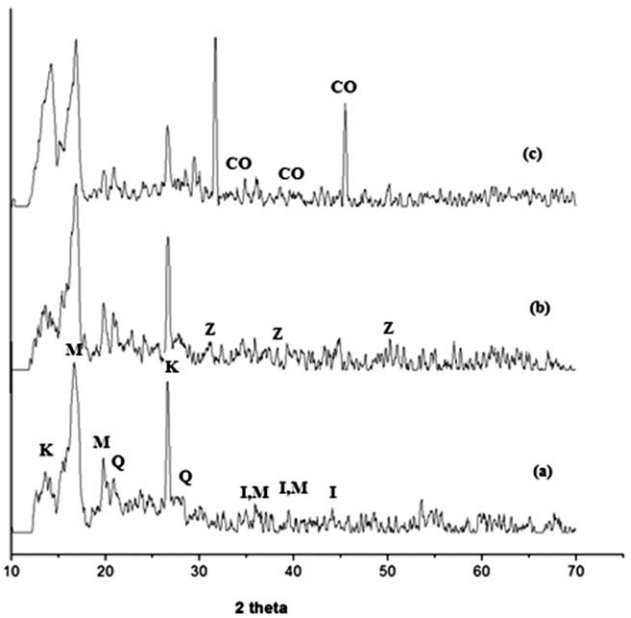

Figure 3. XRD patterns of the original and metal-oxide-impregnated AWBCs: (a) original AWBC, (b) Zn/AWBC, and (c) Co/AWBC (M = montmorillonite, I = illite, Q = quartz, K = kaolinite, Z = ZnO, and Co = Co_2O_3).

Table III. Mineralogical Analysis (wt %) of the Original and Metal-Oxide-Impregnated AWBCs

Mineral	AWBC	Co/AWBC	Zn/AWBC	Ni/AWBC	Fe/AWBC	Mn/AWBC
SiO_2	57.8	46.04	55.16	51.74	49.78	47.12
Al_2O_3	16.5	18.58	15.84	17.20	21.04	23.04
Fe_2O_3	8.5	17.92	5.12	3.20	16.42	3.84
CaO	1.26	1.74	1.26	1.34	1.82	1.00
MgO	1.98	1.60	2.13	1.92	1.85	2.60
Na_2O	2.29	1.29	1.62	1.48	2.02	1.62
K_2O	0.77	0.70	0.72	0.92	0.62	0.65
Co_3O_4	—	8.44	—	—	—	—
ZnO	—	—	12.82	—	—	—
NiO	—	—	—	10.75	—	—
MnO_2	—	—	—	—	—	12.66

also carried out (Table III). The results indicate the presence of Co, Zn, Ni, Fe, and Mn; this confirmed that the precursor metals were effectively impregnated onto plain AWBC.

Acidity measurements were carried out by a titration method. The results are provided in Table IV. The acidity determined in the case of the plain AWBC was found to be 3.2 mg/g; this was increased to the maximum of 4.85 mg/g in the case of Co/AWBC. The results indicate that upon impregnation, the acidity increased, particularly in the case of Co/AWBC and Zn/AWBC.

Activities Tests

The effects of the plain and various impregnated AWBCs on the pyrolysis of the two polyolefins were studied. The overall yields and the yields of liquids, gases, and solid residue as a function of the catalyst type and concentration are provided in Table V. The results indicate that the yields did not change significantly in most of the catalyzed runs when compared with the thermal run. However, in the case of the Co/AWBC- and Zn/AWBC-catalyzed runs, a marginal increase was observed. For instance, in the case of PP, the use of Co/AWBC (1%) caused the total yield to increase up to 99.32 wt %, whereas in the case of HDPE with Zn/AWBC (2.5 wt %), the yield increased up to 99.84 wt %. In the case of the other impregnated AWBCs, the overall yield showed a decrease, which went up to 97 and 70 wt % in the Ni/AWBC-catalyzed runs in the case of PP and HDPE, respectively.

The effects of the plain and impregnated AWBCs on the liquid yields were also studied. The data are provided in Table V. The liquid yields derived from PP and HDPE in the thermal runs were found to be 69.82 and 80.88 wt %, respectively. The results indicated a synergistic effect on the product distribution in the case of the catalyzed runs. We observed that among the catalysts used, Co/AWBC and Zn/AWBC produced a much greater amount of liquids compared to the thermal run. The increase went up to a maximum of 92 wt % in the case of the Co/AWBC (1%)-catalyzed run. Similarly, in the case of HDPE, the liquid yield increased up to 91 wt % in the Zn/AWBC-catalyzed run (2.5%). We inferred from the results that the use of catalysts, particularly impregnated forms, that is, Co/AWBC and Zn/AWBC, caused a significant increase in the liquid yields. The results obtained in the case of the plain and impregnated catalysts show an insignificant effect with increasing concentration.

Table IV. Acidity of the Original and Metal-Oxide-Impregnated AWBCs

Catalyst	Acidity (mg of KOH/g)
AWBC	3.20
Fe/AWBC	4.80
Zn/AWBC	4.20
Ni/AWBC	4.48
Mn/AWBC	4.04
Co/AWBC	4.85

The effects of the AWBCs on the gas yields were also studied. Considerable variations in the gas yields as a function of the catalyst type and concentration were observed from the data compiled in Table IV. A general trend of an increase in the gas yield with an increase in the concentration was observed. The gas yields in the case of the PP and HDPE thermal runs were found to be 28.84 and 17.24 wt %, respectively. The maximum gas yield of 28.24 wt % was achieved in the run catalyzed with Fe/AWBC (10%) in the case of PP; this was comparable with that in the thermal run (28.84 wt %), whereas a yield of 39.91 wt % was achieved in the run catalyzed with Co/AWBC (10%) in the case of HDPE. We observed that most of the catalysts produced insignificant gas yields in the case of PP compared with the thermal run, among which Co/AWBC (1%) gave the lowest yield of 6 wt %. However, in the case of HDPE, the gas yields obtained in most of the catalyzed runs were higher when compared with the thermal run, except in the run catalyzed with Zn/AWBC (5%), which produced the lowest gas yield (8.89%). We observed from the results that the formation of gas was favored with the increase in the concentration of the catalysts used. This indicated that when used in higher concentrations, the catalysts under study might have favored the overcracking reactions and led to the formation of predominantly gas products.

The influence of the catalysts used on the residue/coke was studied, and the data are provided in Table IV. The results indicate that the plain AWBC strongly increased the amount of

Table V. Yields of Pyrolysates (Total Yield and Yields of the Liquid, Gas, and Residue Fractions) Derived from the Thermal and Catalytic Pyrolysis of PP and HDPE Over the Original and Metal-Oxide-Impregnated AWBCs

		Product yield of PP (wt %)				Product yield of HDPE (wt %)			
Catalyst	Catalyst quantity (wt %)	Total yield	Liquid	Gas	Solid residue	Total yield	Liquid	Gas	Solid residue
No catalyst	0	98.66	69.82	28.84	1.34	98.12	80.88	17.24	1.88
	0.5	80.9	60.91	19.99	19.1	79.87	57.46	22.41	20.13
	1	83.13	62.38	20.75	16.87	86.09	67.51	18.58	13.91
AWBC	2.5	84.39	65.76	18.63	15.61	86.93	70.19	16.74	13.07
	5	84.63	68.77	15.86	15.37	79.38	56.63	22.75	20.62
	10	79.72	59.35	20.37	20.28	78.93	55.97	22.96	21.07
Ni/AWBC	0.5	98.12	80.36	17.76	1.6	74.39	46.82	27.57	25.61
	1	99.09	82.91	16.18	0.91	73.61	49.07	24.54	26.39
	2.5	99.33	83.07	16.26	0.67	75.81	58.48	17.33	24.19
	5	99.46	84.97	14.49	0.54	75.77	56.5	19.27	24.23
	10	97.20	77.65	19.55	2.8	70.92	45.89	25.03	29.08
	0.5	98.21	84.36	13.85	1.79	87.5	49.98	37.52	12.5
	1	99.32	92.76	6.56	0.68	87.55	62.07	25.48	12.45
Co/AWBC	2.5	97.70	81.75	15.95	2.30	88.64	69.31	19.33	11.36
	5	96.46	75.66	20.80	3.54	88.33	52.09	36.24	11.67
	10	94.94	73.95	20.99	5.06	87.97	48.06	39.91	12.03
	0.5	96.02	71.46	24.56	3.98	92.14	60.86	31.28	7.86
	1	96.84	82.8	14.04	3.16	92.46	63.05	29.41	7.54
Fe/AWBC	2.5	96.89	82.78	14.11	3.11	93.68	66.36	27.32	6.32
	5	94.61	68.39	26.22	5.39	93.82	71.34	22.48	6.18
	10	92.96	64.64	28.32	7.04	90.56	52.89	37.67	9.44
	0.5	97.99	71.54	26.45	2.01	68.5	42.00	26.50	31.50
	1	98.92	79.23	19.69	1.08	68.5	42.16	26.34	31.50
Mn/AWBC	2.5	99.24	80.4	18.84	0.76	71.76	46.35	25.41	28.24
	5	96.39	69.91	26.48	3.61	73.90	52.71	21.19	26.10
	10	96.21	66.36	29.85	3.79	71.47	43.9	27.57	28.53
	0.5	95.24	75.34	19.90	4.76	97.83	78.6	19.23	2.17
	1	96.91	77.13	19.78	3.09	98.64	81.07	17.57	1.36
Zn/AWBC	2.5	98.40	82.50	15.90	1.60	99.89	91.00	8.89	0.11
	5	94.60	72.89	21.71	5.40	97.50	76.54	20.96	2.50
	10	90.67	68.13	22.54	9.33	94.91	63.11	31.80	5.09

Temperature = 300°C for PP and 350°C for HDPE.

residue, and the impregnation of metal oxide prevented this effect; this was indicative of the fact that the metal-impregnated AWBCs proved effective in decreasing the residue yields by giving rise to more liquid and gas formation.

It is well established that pyrolysis is initiated by the abstraction of the hydride ion (by Lewis acid sites of the catalyst) from the polymer macromolecule or the addition of a proton (by Brönsted acid sites of the catalyst) to the C–C bonds. Successive scissions of the main chain occur to produce fragments having lower molecular weight liquid products. The resulting decomposed fragments are further cracked in the subsequent steps to yield gas products. Such reactions are responsible for the formation of gas, as reported earlier.[33] The high liquid yields in this study indicated the suppression of overcracking reactions by the catalysts under testing.

The variation in liquid yields derived from PP and HDPE could be explained on the same basis. The catalysts under study, particularly Zn/AWBC and CO/AWBC, might have facilitated reactions initiated by the formation of the hydride ion or the addition of a proton due to the inherent acidity or acidity variations incorporated into the AWBC by impregnation with the metal ions. In addition, the role of the surface properties of the catalysts could have also been due to another reason (Table V). Hence, the acidity and pore characteristics appeared to be mainly responsible for the catalytic performance shown by Co/AWBC and Zn/AWBC in terms of producing maximum liquid

yields. The presence of aluminum provided the catalysts with acid properties (Brönsted and Lewis).The difference in acidity was due to the presence of aluminum oxide in different concentrations (Table III). Co/AWBC contained 18.58 wt % aluminum oxide, whereas Zn/AWBC contained 15.84 wt % aluminum oxide. Furthermore, in addition to aluminum oxide, the catalysts were impregnated with Co and Zn, which generated more redox centers and, thereby, caused a change in the acidity.[34]

It was also evident from the results that the liquid yields were quite significant in the case of PP compared to that of HDPE. As reported earlier, the acidic sites present in the catalysts played a vital role in the formation of liquid, gas, and solid residue. The attack by the acidic sites on the main polymer chains yielded oligomers, which underwent the β scission of chain-end carbonium ions and, thereby, formed a gas along with a liquid fraction.[35] Hence, next to acidity, the main polymer chain also had to play a role; thereby, it gave a different product spectrum compared to PP. Co/AWBC especially resulted in a high PP conversion, and Zn/AWBC resulted in a high HDPE conversion. This was due to differences in their topologies. Plastics pose certain specific problems for their catalytic cracking because of both their bulky nature and high viscosity, which create mass-transfer constraints and steric hindrances.[36] There is an anchoring effect associated with certain metal oxides, which prevents the polymer from entering the micropores.[37] Co and Zn might have a low anchoring effect compared to other metal oxides used.

We concluded from the previous discussion that among the impregnated catalysts, Co/BC and Zn/BC exhibited high activities by giving maximum liquid yields in the cases of PP and HDPE, respectively, and were reported to be highly active catalysts for their pyrolysis. An effect of the increase in the concentration was observed only in the case of gas yields, particularly during the pyrolysis of HDPE, where the gas yields were comparable to those in the thermal run; this indicated that the high catalyst polymer ratio did not alter the yields to a great extent. On the basis of the results, we suggest that metal-impregnated AWBCs could be used as active catalysts for the pyrolysis of the polyolefins under study into useful liquid products when used in low concentrations. Several reasons could be possible for the insignificant effect of the increase in the concentrations of the catalysts on the liquid yields; these include the bifunctional nature of the catalysts. It is well established that the activities of bifunctional catalysts are usually associated with the number of the active sites, which are distributed at appropriate distances. When used in higher concentrations, the metal ions dispersed in such a fashion reduce the interaction between the reactants and intermediates[38] and thereby cause poor reaction yields.

Liquid Product Composition

The liquid products derived from PP and HDPE in pyrolysis over Co/AWBC and Zn/AWBC were subjected to compositional analysis by FTIR spectroscopy and GC–MS.

FTIR Analysis. Liquid pyrolysates derived from PP and HDPE in the thermal and catalytic runs were analyzed by FTIR spectroscopy to study their chemical compositions. The results given in Table VI and Figure 4(a–d) indicate that the pyrolysis liquid oils had similar chemical compositions.

The FTIR spectrum of the thermally derived liquid product from PP was provided in Figure 4(a). A number of major and minor absorption peaks with different intensities (weak and strong) in the wave-number range 4000–400 cm^{-1} was observed. Several strong peaks observed in the ranges of 2922, 2852, and 1456 cm^{-1} corresponded to methyl, methylene, and CH_2 bending vibrations, respectively.

The FTIR spectrum of the catalytically derived liquid product is provided in Figure4(b). Several peaks at 2920, 1545, and 1456 cm^{-1} were observed. In a comparison of the results with those of the thermal run, it was evident that the catalyst used did not cause most of the peaks to shift. However, the peak in

Table VI. Major Absorption Peaks and Their Positions, Intensities, and Possible Configurations Assigned in the FTIR Spectra of Liquids Derived from the Thermal and Catalytic Pyrolysis of PP and HDPE

Liquid product	Position (cm^{-1})	Intensity	Assigned configuration
	2922	Strong	CH_3 (aliphatic)
PP thermal run	2852	Strong	CH_2 (aliphatic)
	1456	Strong	CH_2 bending vibrations
	2920	Strong	CH_3 (aliphatic)
Co/AWBC-catalyzed run	1554	Weak	C=C (olefinic)
	1456	Strong	CH_2 bending vibrations
	2920	Strong	CH_3 (aliphatic)
HDPE thermal run	2853	Strong	CH_2 (aliphatic)
	1454	Strong	CH_2 bending vibrations
	2954	Strong	CH_3 (aliphatic)
Zn/AWBC-catalyzed run	2912	Strong	CH_2 (aliphatic)
	1510 and 1550	Medium	C=C (olefinic)
	1456	Strong	CH_2 bending vibrations

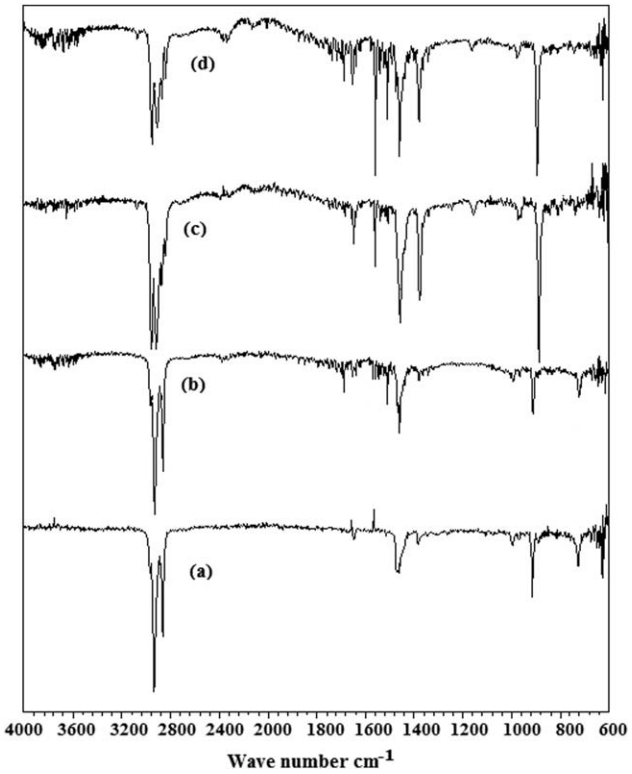

Figure 4. FTIR spectra of the liquid fractions derived from the thermal and catalytic pyrolysis of the polyolefins: (a) PP thermal run, (b) Co/AWBC-catalyzed PP run, (c) HDPE thermal run, and (d) Zn/AWBC-catalyzed HDPE run.

the spectrum of the thermal run at 2852 cm^{-1} was disappeared, and a new peak of weak intensity appeared at 1545 cm^{-1}; this corresponded to C═C.

The FTIR spectrum of the thermally derived liquid product in the case of HDPE is provided in Figure 4(c). Several strong peaks in the wave-number ranges of 2920, 2853, and 1454 cm^{-1} were observed. The FTIR spectrum [Figure 4(d)] of the catalytically derived liquid product from HDPE showed pronounced peaks at 2954, 2912, 1510, 1550, and 1456 cm^{-1}, which indicated CH_3 (aliphatic), CH_2 (aliphatic), C═C (olefinic), and CH_2 bending vibrations. When we compared the spectrum with that of the thermal run, some new peaks positioned at 1510 and 1550 cm^{-1}, which corresponded to C═C (olefinic), were observed. No single peak in the wave-number range corresponding to OH stretching vibrations was observed in any of the spectra; this indicated the absence of water and oxygenates and confirmed that the metal precursors did not react with the BC.

The results confirm the presence of C—CH_3, CH_3, CH═CH, and C—C (ring) groups in all of the derived liquids. Hence, we concluded that the liquid oils mostly consisted of paraffinic, olefinic, and naphthenic hydrocarbons, whereas aromatic and oxygenate functionalities were absent.

Individual Component Analysis. An individual component analysis of the raw/crude liquid pyrolysate derived from PP obtained under the optimum temperature in the case of the thermal run was performed. The GC–MS spectrum is provided in Figure 5(a). The different hydrocarbons identified are listed in Table VII (PP) along with their retention time and percentage peak area. The data were used to deduce the percentage distribution of different carbon range hydrocarbons and hydrocarbon group types in the pyrolysate. We observed that the liquid derived from PP contained naphthenes, olefins, and paraffins with a preponderance of paraffins. Among the naphthenes, the individual molecules identified in high concentrations were 2,4-diethyl-1-methyl cyclohexane, 1-isopropyl-1,4,5-trimethyl cyclohexane, 1-heptyl-2-methyl cyclopropane, and 1,3-dimethyl cyclopentane.

Among the olefins, 1-octene, 4-methyl-2-decene, 5-octadecene E (from entgegen, means opposite), 8-methyl-1-undecene, 1-hexadecene, 1-dodecene, 3-hexadecene, 2-methyl-2-docosene, 1-pentadecene, 1-tetradecene, 5-tetradecene, hexadecene, and heptadecene were the most abundant compounds.

Among the paraffins, hexadecane, tetradecane, pentadecane, heptane, octane, tetratetracontane, 2,6,1,1-trimethyl dodecane, undecane, dodecane, 4,6-dimethyl dodecane, tetradecane, 2,3,5,8-tetramethyl decane, nonadecane, heneicosane, heptadecane, pentatriacontane, docosane, octadecane, tetratriacontane, and octacosane were found in high concentrations.

The GC–MS spectrum of the liquid pyrolysate derived from HDPE at the optimum temperature is provided in Figure 5(b). The individual component molecules identified are presented in Table VIII. Among the naphthenes, 1,1-bieycIohexyl-2-(1-methyl ethyl)-*trans*-1-isopropyl-1,4,5-trimethyl cyclohexane, 1,3,5-trimethyl cyc1ohexane, and eicosyl cyc1ohexane were identified in high concentrations.

Among the olefins, 4,5-dimethyl-2-undecene, 4,5-dimethyl-2-undecene, 3-eicosene (E), 19-eicosadiene, 7-tetradecene (E), 2-ethyl-2-docosene, 1-tricosene, 5-eicosene(E), 1-hexadecene, 4-tetradecene, 2,3,4-trimethyl-1-tricosene, 2,3,4-trimethyl-6-tetradecene, and 1-heptadecene were observed in high concentrations.

Among the paraffins, 2-isopropyl-5-ethyl-1-octane, octacosane, 2,6,10-trimethyl hexadecane, heptadecane, 2-methyl-1-dodecane, 2-heptyl-1-decane, 2-hexyl-1-octane, 2,6,10-trimethyl hexadecane, nonadecane, heneicosane, tetratetracontane, and hexatriacontane were found in high concentrations.

It was evident from the results that the thermally derived liquids in the case of both PP and HDPE were enriched in paraffins followed by olefins followed by naphthenes. No oxygenates and aromatics were observed in either polyolefin.

The main components of the liquid products obtained by the catalytic pyrolysis of PP and HDPE were identified by GC–MS [Figure 5(c,d)]. The results are provided in Tables IX and X. Among the naphthenes identified in the liquid product derived from the Co/AWBC-catalyzed run of PP (Table IX) included 1,3,5-trimethyl cyclohexane, 2,4,6-trimethyl cyclohexane, and 1,1-*trans*-bicyclohexyl-2-(1-methyl ethyl), whereas among the olefins, 2,4-dimethyl heptene, 7-methyl-1-undecene, 4,5-dimethyl-2-undecene, 5-ethyl-2,4-dimethyl 2-heptene, 2,4,6-trimethyl dodecene, and 4-2,3,4-trimethyl tetradecene, were the most abundant compounds. We observed that in the case of PP, the different paraffins identified included heptane, 4-methylheptane, 2,6-dimethyl nonane, dodecane, 2-isopropyl-5-methyl-1-heptane, 2,4-diethyl-1-heptane, and 1-hentetracontane.

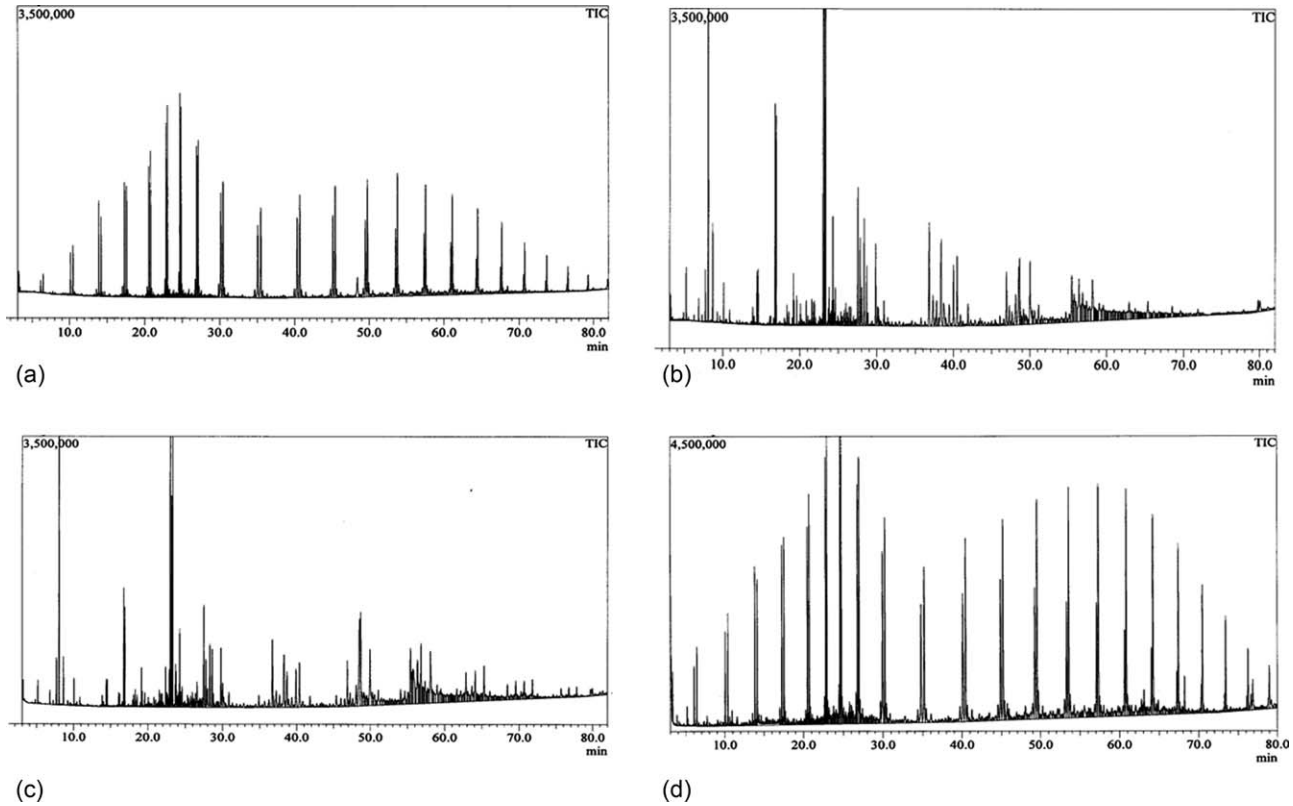

Figure 5. GC–MS spectra of the liquid pyrolysates: (a) PP thermal run, (b) HDPE thermal run, (c) Co/AWBC (1%)-catalyzed PP run, and (d) Zn/AWBC (2.5%)-catalyzed HDPE run.

Similarly, in the case of the Zn/AWBC-catalyzed run of HDPE [Table X and Figure 5(d)], the most occurring compounds among the naphthenes were 1-heptyl-2-methyl cyclopropane and methyl cyclohexane, and the most occurring compounds of the olefins were 1-nonene, 3-hexadecene, 1-dodecene, 1-pentadecene, 1-tetradecene, 1-hexadecene, and 9-tricosene. Among the paraffins, the different compound identified included heptane, octane, nonane, undecane, pentadecane, hexadecane, nonadecane, 2,6,10,14-tetramethyl adecane, and 8-hexyl pentadecane.

C-Number Distribution. The carbon number distributions of the liquid products derived from PP and HDPE were studied by GC–MS analysis. The results are provided in Table XI. In the case of the uncatalyzed run of PP, the yields of different hydrocarbon range products that is, C_6–C_{12}, C_{13}–C_{16}, C_{17}–C_{20}, C_{21}–C_{30} and greater than C_{30}, were found to be 15.16, 33.04, 18.77, 24.97, and 8.05%, respectively. In the case of the Co/AWBC-catalyzed run, the yield of lighter range hydrocarbons, that is, C_6–C_{12}, increased significantly, that is, almost fourfold (60.18%). Similarly, the yield of heavy C-range products, that is, greater than C_{30}, was also increased and attained a value of 12%. On contrary, the yield of middle C-range products decreased significantly. This increase in the yield of light products and the corresponding decrease in the middle-range products was explained on the basis of successive scissions occurring in heavy oligomers, which produced fragments having low molecular weights.

In the case of the liquid product derived from the HDPE thermal run, the yields of different C-range products that is, C_6–C_{12}, C_{13}–C_{16}, C_{17}–C_{20}, C_{21}–C_{30}, and greater than C_{30}, were found to be 32.56, 30.08, 14.19, 12.35, and 10.95%, respectively. In the case of the Zn/AWBC-catalyzed run, the yield of the products, that is, C_6–C_{12}, C_{13}–C_{16}, and C_{17}–C_{20} decreased, whereas the yield of middle and high C-range products (C_{20}–C_{30} and $\geq C_{30}$) increased. This was attributed to the acidic properties of the catalyst used. As reported earlier, the acidic sites present in the catalyst usually attack the main polymer chains and, thereby, yield an oligomer fraction having a carbon range distribution of approximately C_{30}–C_{80}. These oligomers further underwent β scissions of the chain-end carbonium ions; this gave rise to the formation of gas products along with a liquid fraction having a carbon distribution range of approximately C_{10}–C_{25}. In this study, the catalyst used might have favored the formation of heavy hydrocarbons because of the assistance in the oligomer formation from the main polymer. The reduction in light products and the increase in the yield of heavy-range products corresponded to the inactivity exhibited by the catalyst under study toward successive scissions of the high-molecular-weight oligomers; this, in turn, resulted in the production of fragments having high molecular weights.

Hydrocarbon Group Types. The hydrocarbon group type distributions in thermally and catalytically derived liquid products were also studied. The data is compiled in Table XII. We observed that pyrolysis of both polyolefins (PP and HDPE) produced diverse product spectrum in terms of paraffins, olefins and naphthenes.

Table VII. Hydrocarbons Identified in the Liquid Product Derived from the Thermal Pyrolysis of PP

Identification number	Compound	Retention time	Area	Concentration (%)
Naphthene				
1	1,3-Dimethyl cyclopentane	3.041	74,726	1.32
2	1,2-*cis*-Dimethyl cyclopentane	3.091	35,789	0.15
3	1,2-*trans*-Dimethyl cyclopentane	3.142	74,614	0.32
4	Methyl cyclohexane	3.876	4,688	0.16
5	1-Heptyl-2-methyl cyclopropane	13.907	321,308	1.39
6	1-Isopropyl-1,4,5-trimethyl cyclohexane	16.44	2,411	1.61
7	2,4-Diethyl-1-methyl cyclohexane	19.918	2,041	2.03
8	1,1-Bicyclohexyl-2-(1-methyl ethyl)	23.843	32,603	0.14
9	1-Pentanedimethyl cyclohexane	23.843	32,022	0.46
Total yield				7.58
Olefins				
1	1-Octene	6.114	491,287	3.21
2	4-Methyl-2-decene	14.033	452,287	2.48
3	4,5-Dimethyl-2-undecene	17.341	6,521	0.03
4	8-Methyl-1-undecene	18.034	332,826	1.64
5	1-Dodecene	20.58	251,983	1.45
6	5-Tetradecene (E)	20.929	8,828	0.43
7	5-Ethyl-2,4-dimethyl-2-heptene	22.378	27,644	0.64
8	1-Tridecene	22.862	12,089	0.05
9	5-Eicosene (E)	24.019	43,096	0.43
10	3-Hexadecene (Z)	24.683	41,826	0.31
11	2-Methyl-2-docosene	25.467	215,879	1.02
12	1,9-Tetradecadiene	26.704	4,365	0.02
13	1-Pentadecene (E)	26.899	65,065	0.28
14	1-Pentadecene (Z)	30.115	86,131	0.69
15	1-Tetradecene	35.033	224,737	1.27
16	5-Eicosene (E)	39.952	232,012	1.38
17	1-Hexadecene	40.325	245,712	1.55
18	5-Octadecene (E)	41.477	389,739	1.69
19	1,15-Hexadecadiene	44.798	238,225	1.47
20	1-Heptadecene	45.117	59,462	0.26
21	1-Tricosene (E)	45.623	224,958	1.21
22	1-Tricosene (Z)	49.496	36,103	0.13
23	1-Heptadecene	53.535	210,662	1.16
24	5-Nonadecene (Z)	64.268	223,948	1.46
25	2,3,4-Trimethyl-4-tetradecene	65.362	170,589	0.64
26	9-Hexacosene	67.496	8,405	0.24
27	9-Tricosene (Z)	73.553	17,076	0.73
Total yield				25.87
Paraffins				
1	Heptane	3.302	535,428	4.11
2	Octane	6.448	463,611	3.71
3	Nonane	10.453	372,862	2.47
4	Undecane	17.612	513,267	3.23
5	Dodecane	20.799	382,729	2.64
6	4,6-Dimethyl dodecane	22.162	2,917	2.61

Table VII. *Continued*

Identification number	Compound	Retention time	Area	Concentration (%)
7	2,3,5,8-Tetramethyl decane	22.162	2,917	3.21
8	Pentadecane	24.83	1,001,122	4.73
9	4,6-*trans*-Dimethyl dodecane	26.022	3,105	2.61
10	Tetradecane	27.097	1,130,529	4.89
11	2,6,11-Trimethyl dodecane	30.409	116,742	3.45
12	Hexadecane	35.433	1,192,795	5.16
13	Nonadecane	40.678	122,140	2.18
14	Heneicosane	45.431	256,078	1.43
15	Heptadecane	49.768	224,839	1.04
16	2,6,10,14-Tetramethyl hexadecane	53.784	381,003	2.23
17	Docosane	57.544	218,537	1.24
18	Octadecane	61.086	291,331	2.29
19	Tetratetracontane	64.448	828,279	3.58
20	Tetratriacontane	67.658	646,322	2.84
21	Octacosane	70.727	213,943	1.04
22	8-Hexyl pentadecane	73.682	52,518	0.43
23	Hexatriacontane	76.528	220,972	2.56
24	Triacontane	79.274	163,761	2.87
Total yield				66.55

Table VIII. Hydrocarbons Identified in the Liquid Product Derived from the Thermal Pyrolysis of HDPE

Identification number	Compound	Retention time	Area	Concentration (%)
Naphthenes				
1	1,3-Dimethyl cyc1opentane	3.057	93,486	0.38
2	1,2-*cis*-Dimethyl cyc1opentane	3.107	52,474	0.21
3	1,2-*trans*-Dimethyl cyclopentane	3.158	84,691	0.34
4	Methyl cyc1ohexane	3.895	1,540	0.01
5	1,1,3,4-*cis*-Tetramethyl cyc1opentane	6.853	18,391	0.26
6	1,3,5-Trimethy-1-cyc1ohexane	7.726	363,812	1.27
7	Eicosyl cyc1ohexane	16.274	344,829	1.26
8	1-Isopropyl-1,4,5-trimethyl cyc1ohexane	16.625	353,195	1.32
9	2,4-Diethyl-1-methyl cyclohexane	19.628	211,628	0.26
10	1,2-Diethyl-3-methyl cyclohexane	20.11	156,998	0.23
11	1,1-*cis*-Bicyclohexyl-2-(1-methyl ethyl)	23.703	60,034	0.23
12	1-(1,5-Pentanedimethyl) cyclohexane	24.127	32,357	0.18
13	1,1-*trans*-Bieyclohexyl-2-(1-methyl ethyl)	29.841	459,220	2.18
14	l,2-Dibutyl cyclopentane	40.902	19,008	0.27
Total yield				8.40
Olefins				
1	2,4-Dimethyl-1-heptene	8.105	341,146	1.33
2	1-Nonene	10.12	262,186	1.06
3	2,6-Dimethyl-16-octadiene (Z)	10.909	71,853	0.29
4	4-Methyl-2-decene (Z)	14.099	48,230	0.19
5	2,4-Dimethyl-2-decene	16.162	73,198	0.30
6	7-Methyl-1-undecene	16.83	21,155	0.32
7	4,5-Dimethyl-2-undecene	16.971	748,755	3.23

Table VIII. *Continued*

Identification number	Compound	Retention time	Area	Concentration (%)
8	8-Methyl-1-undecene	18.368	84,170	0.34
9	8-Methyl-2-undecene (Z)	18.587	58,123	0.23
10	8-Methyl-3-undecene	19.064	26,476	0.11
11	4,8-Dimethyl-1,7-nonadiene	19.288	145,635	0.59
12	1-Dodecene	20.646	6,045	0.02
13	4,5-Dimethyl-2-undecene	21.064	445,469	2.18
14	5-Ethyl-2,4-dimethyl-2-heptene	22.399	30,047	0.12
15	9-Eicosene (E)	24.051	230,716	1.12
16	5-Eicosene (E)	23.959	25,282	0.14
17	3-Eicosene (E)	24.204	237,970	1.23
18	1,19-Eicosadiene	24.279	344,234	1.36
19	7-Tetradecene (E)	24.933	435,272	2.67
20	2-Ethyl-2-docosene	25.498	325,242	1.74
21	1-Tricosene	28.666	454,829	2.53
22	5-Eicosene (E)	39.999	597,030	2.62
23	1-Hexadecene	40.466	256,475	1.13
24	2,3,4-Trimethyl-4-tetradecene	41.901	211,207	1.45
25	1-Tricosene	46.082	406,665	2.57
26	2,3,4-Trimethyl-6-tetradecene	51.145	151,864	1.61
27	1-Heptadecene	53.558	323,077	1.41
Total yield				31.89
Paraffins				
1	Heptane	3.32	13,484	1.25
2	4-Methyl heptane	5.196	266,917	1.19
3	Octane	6.477	2,448	0.55
4	2,4-Dimethyl heptane	7.30	5,530	0.24
5	2,6-Dimethyl nonane	14.464	210,782	1.29
6	4-Methyl decane	14.612	224,476	1.31
7	Dodecane	20.651	2,619	0.36
8	4,6-Dimethyl dodecane	21.763	103,357	2.42
9	2,3,5,8-Tetramethyl decane	21.916	80,324	1.32
10	2-Isopropyl-5-ethyl-1-octane	23.03	1,411,791	5.44
11	2-Methyl-1-dodecane	23.191	1,111,478	2.44
12	2,4,6-Triethyl-1-dodecane	23.348	37,374	1.36
13	Pentadecane	24.835	9,457	0.44
14	3,6-Dimethyl dodecane	25.983	91,427	1.37
15	3,3,6-Trimethyl decane	26.175	69,610	1.78
16	4,6-Dimethyl dodecane	26.409	90,614	1.45
17	Tetradecane	27.12	37,915	1.47
18	2-Heptyl-1-decane	27.52	584,410	2.46
19	2-Hexyl-1-octane	27.802	422,405	2.73
20	2,6,11-Trimethyl dodecane	30.438	25,354	1.49
21	2,6,10-Trimethyl hexadecane	35.734	316,668	3.21
22	Nonadecane	40.773	22,374	1.38
23	Heneicosane	45.45	629,106	3.62
24	2-Butyl-1-octane	47.325	13,822	0.52
25	2,4-Diethyl-1-heptane	48.158	28,470	0.57

Table VIII. *Continued*

Identification number	Compound	Retention time	Area	Concentration (%)
26	Heptadecane	49.881	415,946	2.25
27	2,6,10,14-Tetramethyl hexadecane	54.002	35,259	1.52
28	Pentatriacontane	55.469	23,566	1.17
29	Docosane	57.586	36,549	1.43
30	Octadecane	61.115	23,434	1.34
31	Tetratetracontane	64.308	14,159	2.32
32	Tetratriacontane	67.671	211,552	0.43
33	Octacosane	70.582	647,800	3.44
34	Hexatriacontane	76.528	220,972	2.63
35	Triacontane	79.274	163,761	1.51
Total yield				59.70

Z = The higher priority groups are on the same side relative to the double bond.

Table IX. Hydrocarbons Identified in the Liquid Product Derived from Catalytic Pyrolysis Over Co/AWBC

Identification number	Name	Retention time	Area	Concentration (%)
Naphthenes				
1	1,3-Dimethyl cyclopentane	3.033	76,667	0.38
2	1,2-*cis*-Dimethyl cyclopentane	3.083	38,469	0.19
3	1,2-*trans*-Dimethyl cyclopentane	3.133	74,764	0.37
4	Methyl cyclohexane	3.861	1,410	0.01
5	1,1,3,4-*cis*-Tetramethyl cyclopentane	6.806	86,838	0.43
6	1,3,5-Trimethyl cyclohexane	7.682	291,904	1.46
7	1,3,5-Trimethyl cyclohexane	8.638	379,493	1.90
8	3,5,5-Trimethyl cyclohexene	9.229	21,054	0.11
9	1-Isopropyl-1,4,5-trimethyl cyclohexane	16.58	41,206	0.21
10	2,4,6-Trimethyl cyclohexane	19.155	271,607	1.36
11	2,4-Diethyl-1-methyl cyclohexane	19.584	118,641	0.59
12	1,2-Diethyl-3-methyl cyclohexane	20.07	70,695	0.35
13	2,4,6-Trimethyl cyclohexane	22.562	49,044	0.25
14	1,1-Bicyclohexyl-2-(1-methyl ethyl)	23.678	248,997	1.25
15	1,1-(1,5-Pentanediyl) biscyclohexane	24.1	74,157	0.37
16	1,2-Dibutyl cyclopentane	40.82	81,488	0.41
Total yield				9.64
Olefins				
17	2,4-Dimethyl heptene	8.045	1,594,791	8.58
18	1-Nonene	10.073	199,468	1.00
19	2,6-Dimethyl-1,6-octadiene (Z)	10.861	54,880	0.27
20	4-Methyl-2-decene (Z)	14.053	34,614	0.17
21	2,4-Dimethyl-2-decene	16.119	140,997	0.71
22	7-Methyl-1-undecene	16.782	483,230	2.42
23	4,5-Dimethyl-2-undecene, R, S (Z)	16.923	391,318	1.96
24	8-Methyl-1-undecene	18.323	78,666	0.39
25	8-Methyl-2-undecene (Z)	18.542	51,080	0.26
26	4,8-Dimethyl-1,7-nonadiene	19.242	104,013	0.52
27	1-Dodecene	21.03	11,293	0.06
28	4,5-Dimethyl-2-undecene, R, R-(E)	21.03	44,195	0.22

Table IX. *Continued*

Identification number	Name	Retention time	Area	Concentration (%)
29	5-Ethyl-2,4-dimethyl-2-heptene	22.369	291,103	1.45
30	9-Eicosene (E)	24.025	29,432	0.15
31	5-Eicosene (E)	23.932	26,208	0.13
32	3-Eicosene (E)	24.176	64,397	0.32
33	1,19-Eicosadiene	24.251	273,695	1.37
34	7-Tetradecene (E)	24.993	4,699	0.02
35	2-Methyl-2-docosene	25.463	37,851	0.19
36	2,3,4-Trimethyl-4-tetradecene	41.813	132,455	0.66
37	1,15-Hexadecadiene	44.488	9,806	0.05
38	1-Tricosene	45.783	9,562	0.05
39	2,4,6-Trimethyl dodecene	49.955	643,328	3.22
40	2,3,4-*cis*-Trimethyl-4-tetradecene	51.073	298,579	1.54
41	2,3,4-Trimethyl-4-tetradecene	65.284	339,643	1.70
42	1,37-Octatriacontadiene	65.653	14,450	0.07
43	2,4,6-Trimethyl-1,1-dodecene	71.809	162,867	0.81
Total yield				28.29
Paraffins				
44	Heptane	3.293	641,780	3.06
45	4-Methyl heptane	5.15	673,664	3.57
46	2,4-Dimethyl heptane	7.253	42,252	0.21
47	2,6-Dimethyl nonane	14.416	478,777	3.89
48	4-Methyl decane	14.565	385,488	2.73
49	Undecane	17.588	5,093	0.03
50	Dodecane	20.616	672,117	3.01
51	5-Methyl-2-(1-methyl ethyl)-1-hexane	21.533	69,396	0.35
52	4,6-Dimethyl dodecane	21.73	68,775	0.34
53	2,3,5,8-Tetramethyl decane	2l.883	54,727	0.27
54	E-10-Pentadecane	22.563	22,643	0.11
55	2-Isopropyl-5-methyl-1-heptane	23	1,155,378	5.78
56	2-Methyl 1-decane	23.16	685,406	3.43
57	2,4-Diethyl-1-heptane	23.317	1,016,413	5.08
58	2-Hexyl-1-decane	23.788	312,965	1.57
59	Isotridecane	25.295	271,186	1.36
60	4,6-Dimethyl dodecane	25.946	69,371	0.35
61	3,3,6-Trimethyl decane	26.136	47,014	0.24
62	6,8-Dimethyl dodecane	26.37	69,545	0.35
63	2-Butyl-1-octane	27.032	13,507	0.07
64	Tetradecane	27.042	60,849	0.30
65	4-Hexyl-1-decane	27.473	512,965	2.57
66	2-Hexyl-1-octane	27.756	280,521	1.40
67	2-Methyl 1-decane	27.963	144,265	0.72
68	3,7,11,15-Tetramethyl-1-hexadecane	28.765	75,163	0.38
69	2,6,11-Trimethyl dodecane	30.37	22,112	0.11
70	Hexadecane	35.367	25,114	0.13
71	1-Pentacontane	36.715	629,277	3.15
72	2,4-Diethyl-1-heptane	38.294	691,197	3.46
73	Nonadecane	40.672	22,231	0.11

Table IX. *Continued*

Identification number	Name	Retention time	Area	Concentration (%)
74	Heneicosane	45.37	67,357	0.34
75	2-Butyl-1-octane	47.248	106,328	0.53
76	3,7,11,15-Tetramethyl-1-hexadecane	47.607	55,828	0.28
77	2,4-Diethyl-1-heptane	48.083	212,063	1.36
78	Heptadecane	49.739	16,301	0.08
79	2,6,10,14-Tetramethyl hexadecane	53.74	19,196	0.10
80	Pentatriacontane	55.399	345,775	1.73
81	Tetrapentacontane	56.336	248,307	1.24
82	1-Hentetracontane	56.806	6,570,743	5.86
83	Docosane	57.514	9,430	0.05
84	Octadecane	61.165	14,267	0.07
85	2-Butyl-1-octane	62.854	212,267	1.46
86	2,4,6,8-Tetramethyl-1-octacosane	63.649	86,784	0.43
87	Tetratetracontane	64.361	10,338	0.05
88	Tetratriacontane	67.629	12,108	0.06
89	Octacosane	70.69	44,625	0.22
90	8-Hexyl pentadecane	73.543	4970	0.02
91	Hexatriacontane	76.553	11,920	0.06
Total yield				62.07

Z = The higher priority groups are on the same side relative to the double bond.
R and S are enantiomers.

Table X. Hydrocarbons Identified in the Liquid Products Derived from the Catalytic Pyrolysis of HDPE Over Zn/AWBC

Identification number	Name	Retention time	Area	Concentration (%)
Naphthenes				
1	1,3-Dimethyl cyclopentane	3.026	45,300	0.22
2	1,2-*cis*-Dimethvl cyclopentane	3.073	37,918	0.18
3	1,2-Dimethyl cyclopentane	3.128	165,014	0.8
4	Methyl cyclohexane	3.851	66,957	0.32
5	1,1,3,4-Tetramethyl cyclopentane	6.957	2,718	0.01
6	1,3,5-Trimethyl cyclohexane	7.336	13,970	0.07
7	1-Heptyl-2-methyl cyclopropane	13.843	714,693	2.27
8	Cyclohexane ecosyl	16.069	5,902	0.03
9	1-Isopropyl-1,4,5-trimethyl cyclohexane	16.28	7,570	0.04
10	2,4,6-Trimethyl cyclohexane	19.077	22,349	0.11
11	2,4-Diethyl-1-methyl cyclohexane	19.509	5,436	0.03
12	1-*trans*-Bicyclohexyl-2-(1-methyl ethyl)	29.657	86,583	0.40
Total yield				4.48
Olefins				
13	1-Octene	6.065	357,197	1.73
14	2,4-Dimethyl-1-heptene	7.988	32,924	0.16
15	1-Nonene	10.062	503,881	2.38
16	4-Methyl-2-decene	14.148	65,311	0.31
17	2,4-Dimethyl-2-decene	16.069	5,081	0.02
18	8-Methyl 1-undecene	18.384	1,655	0.01
19	4,8-Dimethyl-1,7-nonadiene	19.077	22,349	0.11

Table X. *Continued*

Identification number	Name	Retention time	Area	Concentration (%)
20	1-Dodecene	20.508	725,037	3.52
21	5-Tetradecene (E)	20.933	9,463	0.05
22	10-Pentadecene (E)	22.643	136,697	0.66
23	5-Eicosene (E)	23.957	10,443	0.05
24	3-Eicosene (E)	23.957	4,642	0.02
25	1,19-Eicosadiene	23.957	4,642	0.02
26	1-Nonadecene	23.957	4,642	0.02
27	3-Hexadecene (Z)	24.614	1,037,632	4.03
28	2-Methyl-2-docosene	25.54	8,558	0.04
29	1,9-Tetradecadiene	26.597	149,747	0.73
30	1-Pentadecene	26.791	910,681	3.42
31	18-Nonadecene	34.369	125,111	0.61
32	1-Tetradecene	34.788	1,017,790	3.95
33	1-Hexadecene	40.086	877,416	4.26
34	2,4.6-Trimethyl-1,1-dodecene	40.445	326,649	1.50
35	5-Octadecene (E)	41.483	3,653	0.02
36	15-Hexadecadiene	44.562	162,316	0.79
37	1-Tricosene	45.402	93,973	0.46
38	1-Heptadecene	53.725	179,211	0.87
39	5-Nonadecene (Z)	64.348	115,237	1.56
40	11,37-Octatriacontadiene	65.626	55,207	0.26
41	2,3,4-Trimethyl-4-tetradecene	65.308	1,241	0.01
42	9-Hexacosene	67.537	41,034	0.20
43	9-Tricosene (Z)	73.281	114,738	1.56
44	2,4,6-Trimethyl-11-dodecene	71.642	2,258	0.01
Total yield				33.34
Paraffins				
45	Heptane	3.284	339,095	2.65
46	4-Methyl heptane	5.125	13,664	0.07
47	Octane	6.399	870,179	4.31
48	2,4-Dimethyl heptane	7.176	12,658	0.06
49	Nonane	10.395	1,071,671	5.20
50	2,6-Dimethyl nonane	14.612	23,358	0.11
51	4-Methyl decane	14.612	22,876	0.11
52	Undecane	17.541	1,822,935	4.20
53	Dodecane	20.858	39,782	0.19
54	4,6-Dimethyl dodecane	22.1	10,676	0.05
55	2,3,5,8-Tetramethyl decane	22.1	10,676	0.05
56	2-Isopropyl-5-methyl-1-heptane	23.045	75,696	0.48
57	2-Methyl-1-decane	23.22	39,679	0.19
58	2,4-Diethyl-1-heptane	23.22	39,679	0.19
59	2-Hexyl-1-decane	23.957	11,793	0.35
60	Pentadecane	24.843	574,163	2.37
61	Isotridecane	25.291	14,479	0.07
62	4,6-Dimethyl dodecane	25.932	15,823	0.08
63	3,3,6-Trimethyl decane	25.932	13,827	0.07
64	4,6-Dimethyl dodecane	25.932	6,609	0.03
65	Tetradecane	27.101	68,722	0.33

Table X. *Continued*

Identification number	Name	Retention time	Area	Concentration (%)
66	2-Hexyl-1-octane	27.827	11,469	0.06
	1-Tricosene	28.726	789,622	3.04
68	3,7,11,15-Tetramethyl 1-hexadecane	28.614	26,046	0.13
69	2,6,11-Trimethyl dodecane,	30.403	66,932	0.32
70	Hexadecane	35.425	869,895	4.23
71	1-Pentacontane	36.619	14,485	0.07
72	1-Hentetracontane	37.004	28,298	0.17
73	2,4-Diethyl-1-heptane	38.212	45,204	0.37
74	Nonadecane	40.659	146,666	2.67
75	Heneicosane	45.402	763,566	3.60
76	3,7,11,15-Tetramethyl-1-hexadecane	47.911	30,439	0.15
77	Heptadecane	49.724	487,060	2.73
78	2,6,10,14-Tetramethyl hexadecane	53.725	754,583	3.65
79	Pentatriacontane	55.228	31,105	0.15
80	1-Heneicosane	57.471	162,527	2.55
81	Docosane	57.628	35,741	0.17
82	2,3,4-Trimethyl-4-tetradecene	58.778	12,393	0.06
83	Octadecane	61.225	47,380	0.23
84	2-Butyl-1-octane	63.315	22,571	0.11
85	2,4,6,8-Tetramethyl-1-octacosane	63.542	1,926	0.01
86	1-Tetratetracontane	64.348	38,537	0.19
87	Tetratriacontane	67.679	9044	0.04
88	1-Pentacosane	70.315	162,763	2.79
89	Octacosane	70.814	7272	0.04
90	8-Hexyl pentadecane	73.413	1,267,868	6.05
91	Hexatriacontane	76.251	941,288	4.57
92	Triacontane	78.991	585,637	2.84
Total yield				62.15

Z = The higher priority groups are on the same side relative to the double bond.

In the case of the PP thermally derived liquid product, the yields of the paraffins, olefins, and naphthenes were found to be 66.55, 25.87, and 7.58%, respectively. Although in the case of the catalytic run, the yield of paraffins was found to be 62.07%; this was a slight decrease. The yields of olefins and naphthenes were found to be 28.29 and 9.64%, respectively. When we compared the results with those of the thermal run, an increase in olefins and naphthenes was observed. This was attributed to the fact that the catalyst used was a bifunctional one (with Zn as the active ingredient and BC as the support). Supported transition metals have been reported to be highly effective reforming catalysts[39,40] because of their bifunctional nature. These catalysts contain two kinds of active sites that play different roles. The active metals facilitate the hydrogenation reactions, and the acidic sites in the support facilitate reforming reactions. A combination of the two functions may convert plastics into products having a diverse spectrum in terms of paraffins, olefins, naphthenes, and aromatics.[41] The results indicate that the active

Table XI. Carbon Range Distributions in Liquid Products Derived from Thermal and Catalytic Pyrolysis of PP and HDPE

		Distribution (%)				
Polyolefin	Catalyst	C_6-C_{12}	C_{13}-C_{16}	C_{17}-C_{20}	C_{21}-C_{30}	$\geq C_{30}$
	No catalyst	15.16	33.04	18.77	24.97	8.05
PP	Co/AWBC[a]	60.18	16.01	5.06	5.44	12.65
	No catalyst	32.56	30.80	14.19	12.35	10.95
HDPE	Zn/AWBC[b]	30.34	17.46	12.7	22.28	14.64

[a] Catalyst loading = 1%.
[b] Catalyst loading = 2.5%.

Table XII. Hydrocarbon Group Type Distributions in Liquid Products Derived from the Thermal and Catalytic Pyrolysis of PP and HDPE

		Distribution (%)			
Polyolefin	Catalyst	Paraffins	Olefins	Naphthenes	Aromatics
	No catalyst	66.55	25.87	7.58	0.00
PP	Co/AWBC[a]	62.07	28.29	9.64	0.00
	No catalyst	59.70	31.90	8.40	0.00
HDPE	Zn/AWBC[b]	62.15	33.34	4.48	0.00

[a] Catalyst loading = 1%.
[b] Catalyst loading = 2.5%.

metal (Co) played some role in the dehydrogenation and reforming reactions in addition to the active acidic sites present in the support (BC).

In the case of HDPE, the distributions of various hydrocarbon group types, that is, paraffins, olefins, and naphthenes, in the liquid product derived from the thermal run were 59.70, 31.90, and 8.40%, respectively. The yields pattern of paraffinic, olefinic, and naphthenic hydrocarbons obtained during the catalyzed run were 62.15, 33.34, and 4.48%, respectively. In a comparison of the results with those of the thermal run, Zn/AWBC caused an increase in the formation of paraffinic and olefinic hydrocarbons. The yield of naphthenes showed a decrease. The results indicate that in the case of HDPE, the distributions were also affected in the presence of the catalyst. The olefinic intermediates in the case of HDPE, which resulted in the form of the primary cracking products in the catalyzed run, were not easily changed to paraffins by hydrogenation. In addition, the adverse effect on the formation of naphthenes indicated the poor reforming ability of the catalyst used; this was probably due to the nature of the support. As reported elsewhere, polymer cracking is well known to be proceeded by a carbocation mechanism, where the initially formed ions undergo chain reactions via isomerization, β scission, hydrogen transfer, and oligomerization to yield typically light paraffins and olefins.[35] Hence, the catalysts used in this study might have facilitated such reactions and, thereby, gave a product with high concentrations of paraffins and olefins. Olefinic hydrocarbons can influence the properties of fuels, including by increasing the reactivity of gasoline fuels in combustion processes[42] and also by improving the fuel octane number and antiknocking performance.[43] Hence, the high olefinic contents indicated that the derived liquids could be considered as substitute fuels or as feedstocks for obtaining racing fuels.

We observed from the compiled results that the yield of the olefins was high in the PP- and HDPE-derived liquids in the catalyzed runs compared with the thermal run. The results indicate the effectiveness of the catalysts used in terms of enhancement in olefins and naphthenes in the case of PP and paraffins and olefins in the case of HDPE.

CONCLUSIONS

From the previous discussion, the following conclusions were drawn:

- Polyolefins (both PP and HDPE) can be converted more meaningfully into useful liquid products through the catalytic route. Impregnated BCs, particularly Co/AWBC and Zn/AWBC, can be used as catalysts for the conversion of PP and HDPE into value-added products.
- PP can be converted catalytically to produce significant amounts of oilified liquid with a yield as high as 92 wt %.
- HDPE can be converted catalytically to produce significant amounts of oilified liquid with a yield as high as 91 wt %.
- The catalytically derived liquids were enriched in terms of light hydrocarbons in the case of PP and in middle- and heavy-range products as in the case of HDPE, as confirmed from FTIR and GC–MS analyses.
- The catalytically derived liquid in the case of PP was enriched in olefins and naphthenes and in the case of HDPE was enriched in paraffins and olefins.

REFERENCES

1. Ali, S.; Garforth, A. A.; Harris, D. H.; Rawlence, D. J.; Uemichi, Y. *Catal. Today* **2002**, *75*, 247.
2. Miskolczi, N.; Bartha, L.; Deak, G.; Jover, B. *Polym. Degrad. Stab.* **2004**, *86*, 357.
3. Sharratt, P. N.; Lin, Y. H.; Garforth, A. A.; Dwyer, J. *Ind. Eng. Chem. Res.* **1997**, *36*, 5118.
4. Miskolczi, N.; Bartha, L.; Deak, G.; Jover, B.; Kallo, D. *J. Anal. Appl. Pyrol.* **2004**, *72*, 235.
5. Miskolczi, N.; Angyal, A.; Bartha, L.; Valkai, I. *Fuel Process. Technol.* **2009**, *90*, 1032.
6. Lin, Y. H.; Yen, H. Y. *Polym. Degrad. Stab.* **2005**, *89*, 101.
7. Al-Salem, S. M.; Lettieri, P.; Baeyens, J. *Waste Manage.* **2009**, *29*, 2625.
8. Elordi, G.; Olazar, M.; Lopez, G.; Amutio, M.; Artetxe, M.; Aguado, R.; Bilbao, J. *J. Anal. Appl. Pyrol.* **2009**, *85*, 345.
9. Shah, J.; Jan, M. R.; Hussain, Z. *Polym. Degrad. Stab.* **2005**, *87*, 329.
10. Baraniec-Mazurek, I.; Mianowski, A. *Chem. Eng. J.* **2010**, *163*, 284.
11. Jan, M. R.; Shah, J.; Gulab, H. *Fuel* **2010**, *89*, 474.
12. Maher, K. D.; Bressler, D. C. *Bioresour. Technol.* **2007**, *98*, 2351.
13. Siddiqui, M. N. *J. Hazard. Mater.* **2009**, *167*, 728.

14. Elordi, G.; Olazar, M.; Castaño, P.; Artetxe, M.; Bilbao, J. *Ind. Eng. Chem. Res.* **2012**, *51*, 4008.
15. Luo, G.; Suto, T.; Yasu, S.; Kato, K. *Polym. Degrad. Stab.* **2000**, *70*, 97.
16. Manos, G.; Yusof, I. Y.; Papayannakos, N.; Gangas, N. H. *Ind. Eng. Chem. Res.* **2001**, *40*, 2220.
17. Manos, G.; Garforth, A.; Dwyer, J. *Ind. Eng. Chem. Res.* **2000**, *39*, 1203.
18. Kikuchi, E.; Matsuda, T. *Catal. Today* **1988**, *2*, 297.
19. Cheng, S. *Catal. Today* **1999**, *49*, 303.
20. Gyftopoulou, M. E.; Millan, M.; Bridgwater, A. V.; Dugwell, D.; Kandiyoti, R.; Hriljac, J. A. *Appl. Catal. A* **2005**, *282*, 205.
21. Ding, Z.; Kloprogge, J. T.; Frost, R. L. *J. Porous Mater.* **2001**, *8*, 273.
22. Solak, A.; Rutkowski, P. *Waste Manage.* **2014**, *34*, 504.
23. Farshi, R.; Belthur, C.; Athreyas, R.; Jeevan, G. Int. *J. Curr. Eng. Technol.* **2013**, 1(Special Issue, Sept), 172.
24. Shakirullah, M.; Ahmad, I.; Ishaq, M.; Ahmad, W. *Energy Convers. Manage.* **2010**, *51*, 998.
25. Souza, K. R.; deLima, A. F.; deSousa, F. F.; Appel, L. G. *Appl. Catal. A* **2008**, *340*, 133.
26. Vogel, A. I. A Textbook of Quantitative Inorganic Analysis—Theory and Practice; Longmans, Green: London, **2013**.
27. Ahmad, I.; Khan, M. I.; Ishaq, M.; Khan, H.; Gul, K.; Ahmad, W. *Polym. Degrad. Stab.* **2013**, *98*, 2512.
28. Sarkar, M.; Dana, K.; Ghatak, S.; Banerjee, A. *Bull. Mater. Sci.* **2008**, *31*, 23.
29. Ataiwi, A. H.; Abdul-Hamead, A. A. *Emirates J. Eng. Res.* **2012**, *17*, 57.
30. Jovic-Jovicic, N.; Milutinovic-Nikolic, A.; Bankovic, P.; Dojcinovic, B.; Nedic, B.; Gržetic, I.; Jovanovic, D. *Acta Phys. Polonica A* **2010**, *117*, 849.
31. Riad, M.; Mikhail, S. *Catal. Sci. Technol.* **2012**, *2*, 1437.
32. Chang, S. K.; Zainal, Z.; Tan, K. B.; Yusof, N. A. *Sains Malaysiana* **2012**, *41*, 465.
33. Gobin, K.; Manos, G. *Polym. Degrad. Stab.* **2004**, *83*, 267.
34. Barrett, P. A.; Sankar, G.; Catlow, C. R. A.; Thomas, J. M. *J. Phys. Chem.* **1996**; *100*, 8977.
35. Buekens, A. G.; Huang, H. *Res. Conserv. Recycl.* **1998**, *23*, 163.
36. Aguado, J.; Serrano, D. P.; Escola, J. M. *Ind. Eng. Chem. Res.* **2008**, *47*, 7982.
37. Aksoylu, A. E.; Freitas, M. M. A.; Figueiredo, J. L. *Appl. Catal. A* **2000**, *192*, 29.
38. Iglesia, E.; Barton, D. G.; Biscardi, J. A.; Gines, M. J.; Soled, S. L. *Catal. Today* **1997**, *38*, 339.
39. Carnevillier, C.; Epron, F.; Marecot, P. *Appl. Catal. A* **2004**, *275*, 25.
40. Benitez, V.; Boutzeloit, M.; Mazzieri, V. A.; Especel, C.; Epron, F.; Vera, C. R.; Pieck, C. L. *Appl. Catal. A* **2007**, *319*, 210.
41. Lee, K. H.; Noh, N. S.; Shin, D. H.; Seo, Y. *Polym. Degrad. Stab.* **2002**, *78*, 539.
42. Hochhauser, A. M. *SAE Int. J. Fuels Lubs.* **2009**, *2*, 541.
43. Hajbabaei, M.; Karavalakis, G.; Miller. J. W.; Villela, M.; Xu, K. H.; Durbin, T. D. *Fuel* **2013**, *107*, 671.